Published in final edited form as:
J Immunol. 2014 September 15; 193(6): 2931–2940. doi:10.4049/jimmunol.1401151.

Transcriptional profile of TB antigen-specific T cells reveals novel multifunctional features[1]

Cecilia Lindestam Arlehamn[*,2], **Gregory Seumois**[*,2], **Anna Gerasimova**[*], **Charlie Huang**[*], **Zheng Fu**[*], **Xiaojing Yue**[*], **Alessandro Sette**[*], **Pandurangan Vijayanand**[*,†,3], and **Bjoern Peters**[*,3,4]

[*]La Jolla Institute for Allergy & Immunology, La Jolla, CA, 92037, USA

[†] Academic Unit of Clinical and Experimental Sciences, University of Southampton Faculty of Medicine, Sir Henry Wellcome Laboratories, Southampton University Hospital, Southampton SO16 6YD, United Kingdom

Abstract

In latent tuberculosis infection (LTBI) spread of the bacteria is contained by a persistent immune response, which includes $CD4^+$ T cells as important contributors. Here we show that TB-specific $CD4^+$ T cells have a characteristic chemokine expression signature ($CCR6^+CXCR3^+CCR4^-$), and that the overall number of these cells is significantly increased in LTBI donors compared to healthy subjects. We have comprehensively characterized the transcriptional signature of $CCR6^+CXCR3^+CCR4^-$ cells and find significant differences to conventional Th1, Th17 and Th2 cells, but no major changes between healthy and LTBI donors. $CCR6^+CXCR3^+CCR4^-$ cells display linage-specific signatures of both Th1 and Th17 cells, but also have a unique gene expression program including genes associated with susceptibility to TB, enhanced T cell activation, enhanced cell survival, and induction of a cytotoxic program akin to CTL cells. Overall, the gene expression signature of $CCR6^+CXCR3^+CCR4^-$ cells reveals characteristics important for controlling latent TB infections.

INTRODUCTION

Latent tuberculosis infection (LTBI) is characterized by an often life-long containment of mycobacteria to granuloma in the lung that is mediated at least in part by IFNγ producing $CD4^+$ T cells (1). We recently performed a genome-wide screen for epitopes of TB-specific $CD4^+$ T cells (2). Phenotypic characterization of T cells responding to TB-specific epitopes showed that they were remarkably homogenous with more than 80% displaying a $CCR6^+CXCR3^+CCR4^-$ phenotype (2). This T cell subset was independently described by others to be enriched for TB-specific cells (3, 4). These cells have previously been termed Th1 co-expressing CCR6, Th17.1, Th1Th17, Th17/Th1 and Th1/17 cells (2, 5-9), mainly

[1]This work was supported by National Institutes of Health contract HHSN272200900044C (to A.S.), grant U19 AI100275 (to A.S. and B.P.) and R01 HL114093 (to B.P. and P.V.).

[4] Corresponding author: Dr. Bjoern Peters Phone: (858) 752 6914 Fax: (858) 752 6987 bpeters@liai.org.
[2]These authors contributed equally to this work.
[3]Joint senior authors

because they were shown to express both T-bet and RORC (3, 6, 10), the lineage-specific transcription factors of Th1 and Th17 cells, respectively. Yet how these cells differ from conventional Th1 and Th17 cells has not been comprehensively characterized.

Two observations support that TB-specific T cells with this phenotype ($CCR6^+CXCR3^+CCR4^-$) contribute to the containment of TB in LTBI: First, $CCR6^+CXCR3^+CCR4^-$ cells are a preferred target of HIV virus infection, and were shown to be diminished in chronically HIV infected patients (6). The high rate of TB reactivation in HIV patients could thus be a consequence of the reduction in this T cell subset. Second, we and others have shown that TB-specific T cells in LTBI donors are multifunctional and are major producers of TNFα in addition to IFNγ (2, 11). This same phenotype has been described for T cells in rheumatoid arthritis (5, 7), which is treated with TNFα blockers, which in turn has been associated with reactivation of TB (12, 13).

Here, we set out to better characterize the $CCR6^+CXCR3^+CCR4^-$ T cell subset. We find that the frequency of $CCR6^+CXCR3^+CCR4^-$ cells is remarkably expanded in LTBI donors compared to healthy control (HC) donors, and that these cells produce IFNγ, TNFα, IL-2 but no IL-17 upon stimulation with TB derived epitopes. The transcriptional program in TB-specific T cells significantly overlaps with the general $CCR6^+CXCR3^+CCR4^-$ subsets of both LTBI and HC. In addition, we find a unique program of genes, expressed at significantly higher or lower levels in $CCR6^+CXCR3^+CCR4^-$ cells compared to both Th1 and Th17 cells, suggesting that these cells have functional characteristic distinct from either Th1 or Th17 cells. These characteristics are consistent with a multi-functional hyper-activated response program that is persistently maintained and could be required to control latent TB infection.

MATERIALS AND METHODS

Study Subjects

Leukapheresis samples from 12 adults with LTBI and 12 control donors were obtained from the University of California, San Diego Antiviral Research Center clinic (age range 20-65 years). Subjects had a history of a positive tuberculin skin test (TST). LTBI was confirmed by a positive QuantiFERON-TB Gold In-Tube (Cellestis), as well as a physical exam and/or chest X-ray that was not consistent with active tuberculosis. None of the study subjects endorsed vaccination with BCG, or had laboratory evidence of HIV or Hepatitis B. The control donors had a negative TST, as well as a negative QuantiFERON-TB. Research conducted for this study was performed in accordance with approvals from the Institutional Review Board at the La Jolla Institute for Allergy and Immunology (FWA#00000032). All participants provided written informed consent prior to participation in the study.

PBMC Isolation

PBMCs were obtained by density gradient centrifugation (Ficoll-Hypaque, Amersham Biosciences) from 100 ml of leukapheresis sample, according to manufacturer's instructions. Cell were suspended in fetal bovine serum (Gemini Bio-products) containing 10% dimethyl sulfoxide, and cryo-preserved in liquid nitrogen.

Isolation of cells and FACS analysis

HLA class II tetramers conjugated using PE labeled streptavidin were provided by the Tetramer Core Laboratory at Benaroya Research Institute. CD4 T cells were purified using the Miltenyi T cell isolation kit II according to manufacturer's instructions. Purified cells were incubated in PBS containing 0.5% BSA and 2 mM EDTA pH 8.0 (MACS buffer) with a dilution of class II tetramer (10μl tetramer per 50×10^6 CD4 T cells) for 2 h at room temperature. Cells were then stained for cell surface antigens using anti-CD4-APC EFluor780 (RPA-T4), anti-CD45RA-EFluor450 (HI100) (both from Affymetrix eBioscience), anti-CD3-Alexa Fluor 700 (UCHT1), anti-CXCR3(CD183)-APC or CXCR3-Alexa Fluor 488 (1C6/CXCR3), anti-CD19-V500 (HIB19), anti-CD14-V500 (M5E2), anti-CD8-V500 (RPA-T8), anti-CD25-FITC (M-A251), anti-CCR4-PECy7 or CCR4-PE (1G1), anti-CCR6(CD196)-biotinylated (11A9) (all from BD Biosciences) followed by streptavidin-BV605 (BioLegend), anti-CCR7(CD197)-PerCPCy5.5 (G043H7) (BioLegend) and Live/Dead Aqua (Affymetrix eBiosciences) to exclude dead cells. For experiments to evaluate protein expression anti-CCR2(CD192)-PE (K036C2, BioLegend), anti-CD117(KIT)-PE (YB5.B8) and anti-CD117-FITC (104D2), both from Affymetrix eBiosciences were used. Samples were acquired on a BD Aria or LSR II flow cytometer and analyzed using FlowJo software. For phenotyping experiments cells were stained with surface markers as above without the tetramer. For cell sorting cells were sorted into six separate $CD4^+CD3^+CD8/14/19^-CD25^-$ populations; tetramer$^+$, $CCR6^+CXCR3^+CCR4^-$, $CCR6^-CXCR3^+CCR4^-$ (Th1), $CCR6^+CXCR3^-CCR4^-$ (Th17), $CCR6^-CXCR3^-CCR4^+$ (Th2) and $CD4^+CD3^+CD8/14/19^-$ $CD45RA^+CD25^-CCR7^+CXCR3^-CCR6^-CCR4^-$ (naïve) cells (gating strategy in Supplementary figure 1).

For RNAseq of activated cells; $CCR6^+CXCR3^+CCR4^-$ cells were sorted from purified $CD4^+$ T cells on a BD Aria flow cytometer. These and remaining cells (used as antigen presenting cells, APC) were rested over night in complete RPMI medium at 37°C in 5% CO_2. APCs were stained with CFSE according to manufacturer's instruction (Affymetrix eBioscience). Cells were cultured at a ratio of 2:1 $CD4^+$ T cells:APC in the presence of 5 μg/ml TB peptide pool or 0.1 μg/ml PMA with 1 μg/ml Ionomycin for 6 h in complete RPMI medium at 37°C in 5% CO_2. Unstimulated cells were used to assess nonspecific/background activation. After 6 h, cells were harvested and CFSE negative cells ($CCR6^+CXCR3^+CCR4^-$) were sorted from the APCs on a BD Aria flow cytometer.

Intracellular cytokine analysis

$CD4^+$ T cells were purified from PBMCs as above. $CD4^+$ T cells and remaining cells (APC) were rested over night in complete RPMI medium at 37°C in 5% CO_2. Cells were cultured at a ratio of 2:1 $CD4^+$ T cells:APC in the presence of 5 μg/ml TB peptide pool and 4 μg/ml Golgiplug (BD Biosciences) for 6 h in complete RPMI medium at 37°C in 5% CO_2. Unstimulated cells were used to assess nonspecific/background cytokine production. After 6 h, cells were harvested and stained for cell surface antigens CD4, CD3, CD8, CD19, CD14, CXCR3, CCR6, CCR4 and Live/Dead using the same clones and colors as described above. After washing cells were fixed and permeabilized, using a Cytofix/Cytoperm kit (BD Biosciences) and then stained for cytokines using anti-IFNγ-PerCPCy5.5 (4S.B3), anti-TNFα-eFluor 450 (MAb11), anti-IL-17A-PECy7 (eBio64DEC17) and anti-IL-2-FITC

(MQ1-17H12), all from Affymetrix eBioscience. Samples were acquired on a BD LSR II flow cytometer. The frequency of cells responding to the TB-specific peptides was quantified by determining the total number of gated subset+ and cytokine+ cells and background values subtracted (as determined from the medium alone control) using FlowJo software (Tree Star). A cut-off of 2 times the background was used. Combination of cytokine producing cells were determined using Boolean gating in FlowJo software.

Micro-scaled RNA-Sequencing

Total RNA was purified using miRNAeasy kit (Qiagen) and quantified as described previously (14). 10-15ng of purified total RNA was used for poly A section (Poly(A)Purist Mag kit, Lifetechnologies). Poly A selected RNA was amplified with the Whole Transcriptome Amplification Sequencing Technology kit (SEQR, Sigma) as per manufacturers recommendation. One μg of this amplified cDNA was treated with restriction enzyme (SEQR, Sigma), to remove the primer sequences and then purified using AmpureXP beads (Beckman Coulter). Efficiency of removal of SEQR primer sequences was assessed by PCR. From this step, 250 ng of purified DNA was diluted with Te to obtain a total volume of 65 ul. Diluted cDNA was sonicated with E220 Covaris multiplex sonicator (Covaris) to generate 100-250bp DNA fragments. ~ 250 ng of DNA was used for preparing standard SOLiD sequencing library (5500 SOLiD® Fragment 48 Library Core Kit & Fragment Library Barcode Adaptors 1-96). Following emulsion PCR samples were sequenced on the SOLiD 5500 sequencer to obtain 35bp single end reads (SOLiD™ EZ Bead™ E120 System kits). Both, whole transcriptome amplification and sequencing library preparation were performed in a 96-well format, which significantly reduced hands-on time, besides reducing technical and assay-to-assay variability. Multiple quality control steps were included to determine Tot RNA quality and quantity, optimal Poly-A selection, ligation efficiency and number of PCR amplification cycles, to assess removal of whole transcriptome PCR amplification adaptors, shearing of amplified cDNA, fragment size selection, efficiency of ligation of sequencing adaptors and to determine library complexity. Samples that failed QC were eliminated from further downstream steps.

RNA-Seq analysis

The 35bp single end reads were aligned to human hg19 reference genome using the Tophat alignment program (15) allowing reads to span a splice junction. The alignment results were parsed via the samtools package (16) to generate SAM files. In order to quantitatively analyzing the gene expression levels under various cell types and disease types, we only counted the short reads uniquely mapping to an annotated features of the hg19 genome by using htseq-count (17). Here we selected “union” option in htseq-count to deal with reads overlapping more than one feature. After removing absent features (zero counts in all samples), we employed R/Bioconductor package “aroma.light” (18) to perform quantile normalization on the samples for each test (comparison) of differential gene expression. The quantile normalized raw counts were then imported to R/Bioconductor package “DESeq” (19) to identify differentially expressed genes among distinct cell types. We considered genes differentially expressed between two groups of samples if the DESeq analysis resulted in an adjusted p-value < 0.05 and in addition if the fold-change in gene expression was greater two-fold. For genes with low expression close to the detection threshold, normalized

counts <3 were set equal to 3 when calculating fold-change values. Gene Expression Omnibus (GEO) accession code GSE56179 (http://www.ncbi.nlm.nih.gov/geo/).

Statistical analysis

A two-tailed Mann-Whitney test or a one-tailed t-test was used for statistical analysis. Differences with a *P* value of less than 0.05 were considered significant.

RESULTS

TB-epitope-specific memory T cells are predominantly CCR6$^+$CXCR3$^+$CCR4$^-$

Using the T cell library method and TB lysate and peptide pools, it was previously shown that TB-specific memory T cells are predominantly present in the CCR6$^+$CXCR3$^+$CCR4$^-$ memory subset (2, 20). To measure the frequency and distribution of T cells specific for individual TB epitopes, we used a CFP10$_{52\text{-}66}$-DRB5*01:01 tetramer (CFP10$_{52\text{-}66}$; QAAVVRFQEAANKQK) (21). Epitope-specific CD4$^+$ memory T cells including: CD45RA$^-$CCR7$^+$ T$_{CM}$ (central memory), CD45RA$^-$CCR7$^-$ T$_{EM}$ (effector memory), and CD45RA$^+$CCR7$^-$ T$_{EMRA}$ (effector memory expressing CD45RA, Gating strategy in Supplementary figure 1), were detected in 5 LTBI donors at frequencies ranging from 0.022 to 0.519% (median of 0.09, interquartile range 0.03-0.33) (Supplementary figure 2). These cells were not detected in the CD4$^+$ naïve subset or in the CD4$^+$ memory subset from TB uninfected non-BCG vaccinated control donors (healthy controls, HC) (Supplementary figure 2). Next, we investigated the frequency of epitope-specific memory T cells in four memory T cell subsets, defined based on chemokine receptor expression pattern (3) (Supplementary figure 1): CCR6$^+$CXCR3$^+$CCR4$^-$, CCR6$^-$CXCR3$^+$CCR4$^-$ (Th1), CCR6$^+$CXCR3$^-$CCR4$^-$ (Th17), and CCR6$^-$CXCR3$^-$CCR4$^+$ (Th2) cells. As expected from our previous data (2), the epitope-specific CD4$^+$ memory T cells were predominantly present in the CCR6$^+$CXCR3$^+$CCR4$^-$ subset, median 92% of tetramer$^+$ cells (Fig. 1*A*, *B* gating strategy in Supplementary figure 1).

To examine the cytokine profile of these cells, we stimulated CD4$^+$ T cells with TB-specific peptides. These peptides were chosen based on known reactivity in the selected donors all of which were included in the previously described genome-wide epitope screen (2) (Supplementary table I). The responding CCR6$^+$CXCR3$^+$CCR4$^-$ cells are multifunctional and produce IFNγ, TNFα and IL-2 but not IL-17 (Fig. 1*C* and *D*). The majority of CCR6$^+$CXCR3$^+$CCR4$^-$ cells were IFNγ$^+$TNFα$^+$IL-2$^+$ (median 38% of cytokine producing cells), IFNγ$^+$TNFα$^+$ (25%), TNFα$^+$ (18%), followed by TNFα$^+$IL-2$^+$ (12%) and IFNγ$^+$ (3%) (Fig. 1*D*), similar to previous study of TB-specific epitopes (2). This confirms that these cells are a major source of TNFα in line with the hypothesis that TNFα blockers might impede the function of these cells leading to TB reactivation.

CCR6$^+$CXCR3$^+$CCR4$^-$ memory T cells are increased in subjects with LTBI

As TB-specific memory T cells predominantly fall into the CCR6$^+$CXCR3$^+$CCR4$^-$ memory subset, we hypothesized that this subset of T cells could be selectively expanded in LTBI subjects compared to HC. To address this we compared the frequency of CCR6$^+$CXCR3$^+$CCR4$^-$, CCR6$^-$CXCR3$^+$CCR4$^-$ (Th1), CCR6$^+$CXCR3$^-$CCR4$^-$ (Th17),

and $CCR6^{-}CXCR3^{-}CCR4^{+}$ (Th2) memory subsets in LTBI and HC donors. As expected, the fraction of $CCR6^{+}CXCR3^{+}CCR4^{-}$ subset was significantly (p=0.003) increased in LTBI donors with a median of 10.5% compared to 5.5% in HC (Fig. 2*A*, *B*). All other T cell subsets were seen with similar frequencies in the two cohorts; Th1; 16.5%, (LTBI) and 16%, (HC), Th2; 8%, (LTBI) and 8.5%, (HC), and Th17; 5%, (LTBI) and 5%, (HC) (Fig. 2*B* and gating strategy in Supplementary figure 1). These results suggest that the $CCR6^{+}CXCR3^{+}CCR4^{-}$ subset is preferentially expanded following TB infection, and likely to be required for life-long containment of mycobacteria in the host. Further, the presence of this memory subset in healthy subjects with no previous TB exposure or infection indicates that antigen-specific memory T cells to other pathogens may also reside in this subset.

The transcriptional profile of TB-specific memory T cells is similar to $CCR6^{+}CXCR3^{+}CCR4^{-}$ memory subset in LTBI and HC donors

To determine the transcriptional profile of TB-specific memory T cells, we isolated a pure population of $CFP10_{52\text{-}66}$-DRB5*01:01 $tetramer^{+}$ cells from 5 HLA-matched LTBI donors (cell numbers ranging from 10,000 to 70,000). We performed RNA-Seq in these cells and compared them to the broader $CCR6^{+}CXCR3^{+}CCR4^{-}$ memory subset, as well as to the conventional Th1, Th2 and Th17 memory subsets from the same LTBI donors.

Mapping of short mRNA reads to the genome showed that transcripts of the phenotypic markers used for sorting (CXCR3, CCR6 and CCR4) were detectable, and differences in expression levels were consistent with the sorting strategy (Fig. 3*A*). Gene expression values were quantile normalized and pairwise comparisons performed between groups of samples from 4-5 donors each using DESeq (19). We considered a gene as differently expressed if the adjusted p-value was smaller than 0.05 and the change in magnitude of expression was at least two-fold. As expected, we observed increased expression of the two key transcription factors, T-bet and RORC, that are characteristic of Th1 and Th17 cells, respectively, and have both been shown to be expressed in $CCR6^{+}CXCR3^{+}CCR4^{-}$ cells (Fig. 3*B*). This confirms that the sorting strategy and RNA profiling analysis should reliably detect differences in the gene expression profiles of different memory subsets.

Next, we compared the overall transcriptional profiles of different CD4 memory subsets and donor groups. A total of 177 genes met our conservative cutoffs for differential expression when comparing Th1 vs. Th17 cells in LTBI donors (red dots in Fig. 3*B*). A similar number of differences were found when comparing $CCR6^{+}CXCR3^{+}CCR4^{-}$ cells to Th1, Th17 or Th2 cells in LTBI donors (namely 181, 267 and 455, respectively; Fig. 3*C*). The same held true within HC donors (Fig. 3*C*). Thus, there are comparable or more differences in the transcriptional program of $CCR6^{+}CXCR3^{+}CCR4^{-}$ cells compared to any conventional subset as there are between Th1 and Th17 cells.

In contrast, when comparing gene expression in $CCR6^{+}CXCR3^{+}CCR4^{-}$, Th1, Th17 and Th2 cells between LTBI and HC donors, very few differences were detected (0, 2, 0 and 2, respectively; Fig. 3*D*). Finally, when comparing gene expression in Tet^{+} cells to the different T cell subsets, the fewest number of differences were detected in $CCR6^{+}CXCR3^{+}CCR4^{-}$ cells followed by Th1, Th17 and Th2 cells in either LTBI and HC donors (Fig. 3*D*). Overall we concluded that $CCR6^{+}CXCR3^{+}CCR4^{-}$ cells have a

characteristic transcriptional program that distinguishes them from Th1, Th17 and Th2 cells. These characteristics are conserved between LTBI and HC donors, and that TB-specific $CD4^+$ T cells obtained by tetramer sorting in the absence of selection based on surface markers closely resemble $CCR6^+CXCR3^+CCR4^-$ cells.

To analyze the characteristic profiles in more detail, we examined the expression patterns of genes that distinguish $CCR6^+CXCR3^+CCR4^-$, Th1, Th17, Th2 and Tet^+ cells. A total of 1,670 genes were differentially expressed in the pair-wise comparisons made between different cell types and donor groups shown in Figure 3*C* and *D* (for a detailed list of these genes see “Differentially expressed genes” table in GEO submission GSE56179). Figure 4*A* shows a heat map of the expression level of these genes in the different individual samples. When grouping samples based on the similarity of their gene expression pattern by unsupervised clustering, samples from the same cell type fell in separate clusters for Th1, Th2 and Th17 cells, and samples from donors with different disease states were intermixed within those clusters. Samples from $CCR6^+CXCR3^+CCR4^-$ and Tet^+ cells grouped together in one cluster, but there was a tendency of samples from LTBI donors and HC donors to separate within this cluster and for the Tet^+ samples to be more similar to samples from LTBI donors.

Given that the same donors were the source of Tet^+ and $CCR6^+CXCR3^+CCR4^-$ LTBI samples, caution has to be applied when interpreting the increased similarity of TB-specific Tet^+ cells with $CCR6^+CXCR3^+CCR4^-$ cells in TB infected individuals. Still, given the significant expansion of the $CCR6^+CXCR3^+CCR4^-$ subset in LTBI donors, it is possible that Tet^+ cells constitute a specialized subset of cells within the $CCR6^+CXCR3^+CCR4^-$ compartment that have a differential expression pattern for a subset of genes.

$CCR6^+CXCR3^+CCR4^-$ cells display hallmarks of both Th1 and Th17 transcriptional programs

A total of 357 genes were differentially expressed in Th1 vs. Th17 cells when comparing groups of either HC or LTBI donors. When examining the expression profile of these genes in $CCR6^+CXCR3^+CCR4^-$ cells, most showed a pattern similar to Th1 cells (172 genes, 48%), a sizeable fraction showed an intermediate expression level (128 genes, 36%), and comparably fewer genes displayed a pattern similar to Th17 cells (57 genes, 16%). Notably, the lineage-specific transcription factor T-bet (*TBX21*) of Th1 cells was upregulated in both $CCR6^+CXCR3^+CCR4^-$ and Th1 cells compared to Th17 cells, as well as several cytotoxic factors such as granzymes A, K, perforin (*PRF1*), and the transcription factor *EOMES* (Fig. 4*B*). Yet, granzyme B and M were exclusively upregulated in Th1 cells and consistently lower in both Th17 and $CCR6^+CXCR3^+CCR4^-$. Conversely, the lineage-specific Th17 transcription factor RORC was upregulated in both $CCR6^+CXCR3^+CCR4^-$ and Th17 cells compared to Th1 cells along with other Th17-selective genes such as *ADAM12*, *PTPN13* and *IL17RE*, the receptor for IL17C. *IKZF2* (Ikaros) however, was upregulated in Th17 (and Th2) cells but not in $CCR6^+CXCR3^+CCR4^-$ and Th1 (Fig. 4*B*). Overall, this confirms that $CCR6^+CXCR3^+CCR4^-$ cells show hallmarks of both Th1 and Th17 expression and that within the signature genes differentiating Th1 cells from Th17 cells, the expression pattern more closely resembles that of Th1 cells.

CCR6$^+$CXCR3$^+$CCR4$^-$ cells selectively express genes associated with TB susceptibility and enhanced T cell persistence

All previously published analyses of the transcriptional program of CCR6$^+$CXCR3$^+$CCR4$^-$ cells have focused on candidate genes of interest most of which were known to play a role in T cell linage development, such as RORC and T-bet. Here, we analyzed in an unbiased fashion which genes are expressed differentially in CCR6$^+$CXCR3$^+$CCR4$^-$ cells as compared to the conventional CD4 memory subsets: Th1, Th17 and Th2 cells. We considered a gene to be differentially expressed in CCR6$^+$CXCR3$^+$CCR4$^-$ cells if its median expression level was consistently at least 2-fold higher (or lower) than its median expression level in either Th1, Th17 or Th2 cells. We included genes if they met these criteria in either LTBI or HC donors. A total of 412 genes met these criteria, with 203 of them increased and 209 decreased in CCR6$^+$CXCR3$^+$CCR4$^-$ subset, as compared to the other T cell subsets (Fig. 4). Pathway analysis of CCR6$^+$CXCR3$^+$CCR4$^-$-specific upregulated genes showed enrichment of genes related to Cytokine:Receptor interactions (*CCR2*, *IL12RB2*, *IL23R*, *KIT* (CD117, c-KIT), *BAFF* (CD257, TNFSF13B)) (Fig. 4*B*). The increased expression of genes involved in cell survival and proliferation (*i.e. BAFF*, *MDR1 (ABCB1)* and *KIT*) suggests that the CCR6$^+$CXCR3$^+$CCR4$^-$ cells may represent a highly persistent memory population. Further, other genes with increased expression (*CCR2* and *IL12RB2*) have been linked to TB susceptibility, (22, 23), supporting the notion that CCR6$^+$CXCR3$^+$CCR4$^-$ cells are important for control of TB infection.

The list of genes downregulated in CCR6$^+$CXCR3$^+$CCR4$^-$ cells includes TIGIT (Fig. 4*B*), a surface protein that has T-cell intrinsic regulatory inhibitory function. Impairment of this function is associated with increased T cell persistence and immunoreactivity (24). Also, CCR6$^+$CXCR3$^+$CCR4$^-$ cells have significantly lower expression of ThPOK (Fig. 4*B*), loss of which has been described to result in derepression of aspects of the gene-expression program of the CD8+ cytotoxic T lymphocyte (CTL) lineage, resulting in cytotoxic activity of CD4+ T cells (25). Overall, CCR6$^+$CXCR3$^+$CCR4$^-$ cells display lineage-specific signatures of both Th1 and Th17 cells, but also have a unique gene expression program including genes associated with susceptibility to TB, enhanced T cell activation, enhanced cell survival, and induction of a cytotoxic program akin to CTL cells, suggesting a highly potent and multifunctional T cell subset.

CCR6$^+$CXCR3$^+$CCR4$^-$ cells produce a broad spectrum of cytokines upon activation

As shown in Figure 1, upon stimulation with T cell epitopes from TB, CCR6$^+$CXCR3$^+$CCR4$^-$ cells from LTBI donors produced IFNγ, TNFα and IL-2. To more broadly examine the functional profile of these cells, we stimulated CCR6$^+$CXCR3$^+$CCR4$^-$ cells from three LTBI donors with PMA/ionomycin and compared their transcriptional profile to resting CCR6$^+$CXCR3$^+$CCR4$^-$ cells. We specifically examined change of expression for a panel of 52 cytokines including all that have been previously reported to be produced by human T cells in an epitope specific manner (26). Figure 5 shows all cytokines in the panel that showed a greater than 3-fold induction of expression after PMA/Ionomycin stimulation. As expected, the production of *IFNG*, *TNF* and *IL2* could reliably be detected also at the transcript level. In addition a large number of cytokines were produced upon stimulation by CCR6$^+$CXCR3$^+$CCR4$^-$ cells namely *CSF1/2*, *CCL3/4*, *GZMB*, *IL6/17A/22*,

CXCL9 and *VEGFA*. CSF1 (M-CSF) and CSF2 (GM-CSF) play a major role in differentiation, survival and enhancing the anti-microbial activity of macrophages (27, 28). CSF-1 has also been shown to play a role in the adaptive immune response against TB (29). Interestingly, mutations in the *CCL4* (30) and *IL22* (31) loci have been associated with increased susceptibility to TB. Overall, these data reinforce that $CCR6^+CXCR3^+CCR4^-$ cells are capable of producing a broad spectrum of cytokines that contribute to their ability to contain LTBI.

Protein expression pattern of $CCR6^+CXCR3^+CCR4^-$ signature genes

Next, we determined if the unique transcriptional profile of $CCR6^+CXCR3^+CCR4^-$ cells was reflected in a similar expression profile at the protein level. $CD4^+$ cells from HC and LTBI donors were examined for the surface expression of CCR2 and KIT. Both markers were expressed at significantly higher levels in $CCR6^+$ (CCR2 median 49.8%, KIT 5.8%) vs. $CCR6^-$ (CCR2 17.0%, KIT 0.5%) (Fig. 6*A*). As was predicted from the transcriptional profile, expression was significantly increased in the $CCR6^+CXCR3^+CCR4^-$ cells (CCR2 58.4%, KIT 7.1%) compared to the other CD4 memory subsets: Th1 (CCR2 27.2%, KIT 1.0%), Th17 (CCR2 31.7%, KIT 2.0%) and Th2 (CCR2 14.2%, KIT 0.6%) (Fig. 6*A*).

The expression of CCR2 and KIT was also investigated in TB-specific cells by co-staining cells with the DRB5*01:01 CFP10 tetramer (Fig. 6*B*). Interestingly, the majority of TB-epitope-specific cells expressed CCR2 (92.0%), but was negative for KIT (94.9%) (Fig. 6*C*). Selection of $CCR2^+$ cells within $CCR6^+CXCR3^+CCR4^-$ cells results in around 45% increase of $tetramer^+$ and thus TB-specific cells (Fig. 6*D*). The exclusion of KIT $^+$ cells had only a minor effect, with 2.3% increase. Thus, the transcriptional profile pinpointed additional markers expressed by the $CCR6^+CXCR3^+CCR4^-$ T cell subset and at the same time suggested that this subset is heterogeneous in terms of expression of markers characteristic of T cell activation and differentiation.

Discussion

Previous studies of TB-specific transcriptional signatures used whole blood rather than sorted T cell populations (32-37). While useful for e.g. diagnostic purposes, the mechanistic interpretation of the appearance of a new transcriptional signature in whole blood is complicated in that it does not distinguish between changes in gene expression in the same cells from changes in composition of cells in the blood. Here we show that, strikingly, the gene expression profile in different T cell subsets is essentially unchanged between healthy and latently infected individuals. However, in latently infected donors there is an expansion of the particular set of memory T cells that are TB-specific. Thus, differences in CD4 T cell gene expression between LTBI and healthy donors are primarily a result of a change in the relative frequency of different CD4 subsets.

$CD4^+$ memory T cell subsets are defined by the coordinate expression of selected cytokines, chemokine receptors and transcription factors. The well-characterized subsets Th1, Th2 and Th17 can be distinguished based on their expression of CXCR3, CCR6 and CCR4 (38). Here, using these chemokine receptors as markers we have characterized a subset of cells that express CXCR3 and CCR6 but not CCR4. Similar cells had been previously shown to

express the hallmark transcription factors of both Th1 and Th17 cells namely T-bet and RORC (3, 6, 10) and have consequently been referred to as Th1 co-expressing CCR6, Th17.1, Th1Th17, Th17/Th1 and Th1/17 cells (2, 5-9). However, our in-depth analysis of the transcriptional signature of $CXCR3^+CCR6^+CCR4^-$ cells suggests that they are associated with a characteristic transcriptional profile that sets them apart from both Th1 and Th17 cells.

Our original interest in $CCR6^+CXCR3^+CCR4^-$ cells was triggered by our finding that TB-specific $CD4^+$ T cells in LTBI donors fall nearly exclusively into this subset. These cells are remarkable in that they can easily be detected directly *ex vivo* due to their ability to mount a strong multifunctional response to their cognate antigens. Multiple lines of evidence suggest that TB-specific memory cells are necessary for the often life-long containment of TB in latent infection (39-42). Adding to this evidence, we found here that the number of cells in the $CCR6^+CXCR3^+CCR4^-$ subset is greatly increased in LTBI (and by definition asymptomatic) donors. This study was completed in a non-TB-endemic population. Ongoing studies include a larger cohort from different ethnicities, locations, disease states, and BCG vaccination status. This will provide answers pertaining to this subset and transcriptional signatures in patients from an endemic area or with different disease states. Our transcriptional analysis revealed that $CCR6^+CXCR3^+CCR4^-$ cells preferentially express CCR2 and IL12 receptor and upon activation produce large amounts of CCL4 and IL-22, all of which have been implicated in higher susceptibility to TB infection (22, 23, 30, 31). Understanding the characteristics of $CCR6^+CXCR3^+CCR4^-$ cells that provide them with the ability to contain TB infection should in turn provide better correlates of efficacy for TB vaccine development, which are currently lacking, and might also suggest specific pathways that can be exploited for development of antimycobacterial drugs.

Previous reports on $CCR6^+CXCR3^+CCR4^-$ cells (or cells sorted on some but not all of the markers $CXCR3^+$, $CCR6^+$ and $CCR4^-$) have shown that such cells can produce IL-17 upon *in vitro* expansion (3, 5, 8). We did not detect IL-17 production of TB-specific $CCR6^+CXCR3^+CCR4^-$ cells upon *ex vivo* antigen-specific stimulation. The lack of ability to detect TB-specific IL-17 producing $CCR6^+CXCR3^+CCR4^-$ cells is in agreement with a previous study (3), in which $CCR6^+CXCR3^+CCR4^-$ cells stimulated with TB protein extract (PPD) for five days did not produce IL-17, while $CCR6^+CXCR3^+CCR4^-$ cells stimulated with Candida extract under identical conditions did. This suggests that a subset of $CCR6^+CXCR3^+CCR4^-$ cells is responsible for IL-17 production, and our ability to detect some IL-17 expression in bulk $CCR6^+CXCR3^+CCR4^-$ cells from LTBI donors after PMA/ionomycin stimulation is in agreement with this conclusion. Given that $CCR6^+CXCR3^+CCR4^-$ cells showed a slight separation in the gene expression profile between HC and LTBI donors supports the notion that markers could be defined discriminating $CCR6^+CXCR3^+CCR4^-$ cells that produce IL-17 from those that do not, the latter being presumably enriched in LTBI donors. However, while there may be some differences between $CCR6^+CXCR3^+CCR4^-$ cells in HC and LTBI donors, many more commonalities exist, especially in comparison to conventional Th1, Th2 and Th17 cells, suggesting an overarching shared transcriptional program in $CCR6^+CXCR3^+CCR4^-$ cells.

Within the shared transcriptional program that distinguishes $CCR6^+CXCR3^+CCR4^-$ cells from other memory subsets, several genes were indicative of $CCR6^+CXCR3^+CCR4^-$ cells showing increased immune-activation after prolonged stimulation. $CCR6^+CXCR3^+CCR4^-$ cells express significantly higher levels of CCR2 and the TB-specific cells are almost exclusively CCR2 positive. CCR2 has been described as a marker of terminally differentiated T cells that is the result of multiple antigen encounters (43), which in the case of TB-specific cells is likely the outcome of chronic stimulation in LTBI donors. Furthermore, $CCR6^+CXCR3^+CCR4^-$ cells lack expression of TIGIT which has been shown to result in hyperproliferative T cell responses (24). Finally, $CCR6^+CXCR3^+CCR4^-$ cells have significantly lower expression of the master transcription factor ThPOK. Down-regulation of ThPOK expression in mouse CD4 T cells coincides with chronic activation and results in loss of the Th-program and the gain of a gene expression program typical of CTL (25). $CD4^+$ CTL cells have been described previously in the context of infectious diseases (44-46). Overall, this expression profile is consistent with the hypothesis that $CCR6^+CXCR3^+CCR4^-$ cells have undergone multiple rounds of antigen stimulation and in that course overcome intrinsic barriers that normally reduce the responsiveness of T cells, making them effective controllers of persistent or recurrent infections.

$CCR6^+CXCR3^+CCR4^-$ cells are persistently present in LTBI donors in large numbers. This could be the result of increased longevity of these cells, which is consistent with the observed gene expression signature as $CCR6^+CXCR3^+CCR4^-$ cells selectively express MDR1. MDR1 is associated with survival and longevity of cells (47, 48). Also, *KIT* is expressed significantly higher on the $CCR6^+CXCR3^+CCR4^-$ as compared to all other T cell subsets and is associated with enhanced cell survival (5), as is the transcription of BAFF (49). Alternatively, the persistent presence of $CCR6^+CXCR3^+CCR4^-$ cells could also be the result of them being constantly replenished from a yet-to-be identified progenitor population.

In reviewing the literature on $CCR6^+CXCR3^+CCR4^-$ cells and genes associated with their unique transcriptional program, several reports implicated these cells and genes in chronic inflammatory autoimmune diseases such as rheumatoid arthritis (RA) and Crohn's disease (5, 7, 9, 50). The exact properties that make $CCR6^+CXCR3^+CCR4^-$ cells desirable to control infections may make them particularly harmful as disease causing cells in autoimmune and other inflammatory diseases. Thus, the genes discovered here as uniquely associated with $CCR6^+CXCR3^+CCR4^-$ cells may not only be useful to better identify what genes should be induced by vaccination, but also what genes could potentially be targeted to treat autoimmunity and inflammation.

The origin of $CCR6^+CXCR3^+CCR4^-$ remains to be defined. A previous study of T cells enriched in the joints of rheumatoid arthritis patients showed that these cells have a $CCR6^+CCR4^-$ phenotype, and are derived from conventional Th17 T cells, as assessed by a shared TCR repertoire (7). Furthermore, the authors showed that Th17 cells can be converted *in vitro* to this phenotype by culturing them in the presence of IL-12, as was also previously shown (9). This suggests that there is a pathway for Th17 cells to differentiate towards the multifunctional $CCR6^+CXCR3^+CCR4^-$ CTL-like phenotype. Other studies suggest that $CCR6^+CXCR3^+CCR4^-$ may also arise from Th1 cells (8). It therefore remains

to be seen if the $CCR6^{+}CXCR3^{+}CCR4^{-}$ cells are a separate lineage or similar to the ThPOK negative CD4 CTL in mice, represent an advanced state of differentiation for cells of different origin including both Th1 and Th17 cells.

In conclusion, this study describes the transcriptional signature of $CCR6^{+}CXCR3^{+}CCR4^{-}$ to an unprecedented level of detail. Our results suggest that $CCR6^{+}CXCR3^{+}CCR4^{-}$ cells are important in controlling chronic/latent infections and also play a role in pathogenesis and drug resistance of autoimmune diseases. Furthermore, they represent a persistent human T cell subset, thus may be important to understanding mechanisms of long-term immune memory and vaccine responses. These cells and their transcriptional signature may be exploited to improve diagnosis, characterization and treatment of not only TB patients but ultimately also patients with inflammatory diseases.

Supplementary Material

Refer to Web version on PubMed Central for supplementary material.

Abbreviations

CFP10	culture filtrate protein 10kDa
HC	healthy control
LTBI	latent tuberculosis infection
TB	tuberculosis
Tet	tetramer
TST	tuberculin skin test

REFERENCES

1. Flynn JL, Chan J. IMMUNOLOGY OF TUBERCULOSIS. Annu Rev Immunol. 2001; 19:93–129. [PubMed: 11244032]
2. Lindestam Arlehamn CS, Gerasimova A, Mele F, Henderson R, Swann J, Greenbaum JA, Kim Y, Sidney J, James EA, Taplitz R, McKinney DM, Kwok WW, Grey H, Sallusto F, Peters B, Sette A. Memory T Cells in Latent Mycobacterium tuberculosis Infection Are Directed against Three Antigenic Islands and Largely Contained in a CXCR3+CCR6+ Th1 Subset. PLoS Pathog. 2013; 9:e1003130. [PubMed: 23358848]
3. Acosta-Rodriguez EV, Rivino L, Geginat J, Jarrossay D, Gattorno M, Lanzavecchia A, Sallusto F, Napolitani G. Surface phenotype and antigenic specificity of human interleukin 17-producing T helper memory cells. Nat. Immunol. 2007; 8:639–646. [PubMed: 17486092]
4. Perreau M, Rozot V, Welles HC, Belluti-Enders F, Vigano S, Maillard M, Dorta G, Mazza-Stalder J, Bart PA, Roger T, Calandra T, Nicod L, Harari A. Lack of Mycobacterium tuberculosis-specific interleukin-17A-producing CD4+ T cells in active disease. Eur J Immunol. 2013; 43:939–948. [PubMed: 23436562]
5. Ramesh R, Kozhaya L, McKevitt K, Djuretic IM, Carlson TJ, Quintero MA, McCauley JL, Abreu MT, Unutmaz D, Sundrud MS. Pro-inflammatory human Th17 cells selectively express P-glycoprotein and are refractory to glucocorticoids. J Exp Med. 2014; 211:89–104. [PubMed: 24395888]
6. Gosselin A, Monteiro P, Chomont N, Diaz-Griffero F, Said EA, Fonseca S, Wacleche V, El-Far M, Boulassel MR, Routy JP, Sekaly RP, Ancuta P. Peripheral blood CCR4+CCR6+ and

CXCR3+CCR6+CD4+ T cells are highly permissive to HIV-1 infection. Journal of immunology. 2010; 184:1604–1616.

7. Nistala K, Adams S, Cambrook H, Ursu S, Olivito B, de Jager W, Evans JG, Cimaz R, Bajaj-Elliott M, Wedderburn LR. Th17 plasticity in human autoimmune arthritis is driven by the inflammatory environment. Proc Natl Acad Sci U S A. 2010; 107:14751–14756. [PubMed: 20679229]
8. Cohen CJ, Crome SQ, MacDonald KG, Dai EL, Mager DL, Levings MK. Human Th1 and Th17 cells exhibit epigenetic stability at signature cytokine and transcription factor loci. J Immunol. 2011; 187:5615–5626. [PubMed: 22048764]
9. Annunziato F, Cosmi L, Santarlasci V, Maggi L, Liotta F, Mazzinghi B, Parente E, Fili L, Ferri S, Frosali F, Giudici F, Romagnani P, Parronchi P, Tonelli F, Maggi E, Romagnani S. Phenotypic and functional features of human Th17 cells. J Exp Med. 2007; 204:1849–1861. [PubMed: 17635957]
10. Zielinski CE, Mele F, Aschenbrenner D, Jarrossay D, Ronchi F, Gattorno M, Monticelli S, Lanzavecchia A, Sallusto F. Pathogen-induced human TH17 cells produce IFN-gamma or IL-10 and are regulated by IL-1beta. Nature. 2012; 484:514–518. [PubMed: 22466287]
11. Wilkinson KA, Wilkinson RJ. Polyfunctional T cells in human tuberculosis. European Journal of Immunology. 2010; 40:2139–2142. [PubMed: 20853500]
12. Galloway JB, Hyrich KL, Mercer LK, Dixon WG, Fu B, Ustianowski AP, Watson KD, Lunt M, Symmons DP. Anti-TNF therapy is associated with an increased risk of serious infections in patients with rheumatoid arthritis especially in the first 6 months of treatment: updated results from the British Society for Rheumatology Biologics Register with special emphasis on risks in the elderly. Rheumatology (Oxford). 2011; 50:124–131. [PubMed: 20675706]
13. Keane J, Gershon S, Wise RP, Mirabile-Levens E, Kasznica J, Schwieterman WD, Siegel JN, Braun MM. Tuberculosis Associated with Infliximab, a Tumor Necrosis Factor α–Neutralizing Agent. New England Journal of Medicine. 2001; 345:1098–1104. [PubMed: 11596589]
14. Seumois G, Vijayanand P, Eisley CJ, Omran N, Kalinke L, North M, Ganesan AP, Simpson LJ, Hunkapiller N, Moltzahn F, Woodruff PG, Fahy JV, Erle DJ, Djukanovic R, Blelloch R, Ansel KM. An integrated nano-scale approach to profile miRNAs in limited clinical samples. American journal of clinical and experimental immunology. 2012; 1:70–89. [PubMed: 23304658]
15. Trapnell C, Pachter L, Salzberg SL. TopHat: discovering splice junctions with RNA-Seq. Bioinformatics. 2009; 25:1105–1111. [PubMed: 19289445]
16. Li H, Handsaker B, Wysoker A, Fennell T, Ruan J, Homer N, Marth G, Abecasis G, Durbin R, S. Genome Project Data Processing. The Sequence Alignment/Map format and SAMtools. Bioinformatics. 2009; 25:2078–2079. [PubMed: 19505943]
17. Anders S, Pyl PT, Huber W. HTSeq - A Python framework to work with high-throughput sequencing data. bioRxiv. 2014
18. Bengtsson H, Ray A, Spellman P, Speed TP. A single-sample method for normalizing and combining full-resolution copy numbers from multiple platforms, labs and analysis methods. Bioinformatics. 2009; 25:861–867. [PubMed: 19193730]
19. Anders S, Huber W. Differential expression analysis for sequence count data. Genome Biol. 2010; 11:R106. [PubMed: 20979621]
20. Geiger R, Duhen T, Lanzavecchia A, Sallusto F. Human naive and memory CD4+ T cell repertoires specific for naturally processed antigens analyzed using libraries of amplified T cells. J Exp Med. 2009; 206:1525–1534. [PubMed: 19564353]
21. Lindestam Arlehamn CS, Sidney J, Henderson R, Greenbaum JA, James EA, Moutaftsi M, Coler R, McKinney DM, Park D, Taplitz R, Kwok WW, Grey H, Peters B, Sette A. Dissecting Mechanisms of Immunodominance to the Common Tuberculosis Antigens ESAT-6, CFP10, Rv2031c (hspX), Rv2654c (TB7.7), and Rv1038c (EsxJ). The Journal of Immunology. 2012; 188:5020–5031. [PubMed: 22504645]
22. Peters W, Scott HM, Chambers HF, Flynn JL, Charo IF, Ernst JD. Chemokine receptor 2 serves an early and essential role in resistance to Mycobacterium tuberculosis. Proc Natl Acad Sci U S A. 2001; 98:7958–7963. [PubMed: 11438742]
23. Casanova J-L, Abel L. GENETIC DISSECTION OF IMMUNITY TO MYCOBACTERIA: The Human Model. Annu Rev Immunol. 2002; 20:581–620. [PubMed: 11861613]

24. Joller N, Hafler JP, Brynedal B, Kassam N, Spoerl S, Levin SD, Sharpe AH, Kuchroo VK. Cutting edge: TIGIT has T cell-intrinsic inhibitory functions. J Immunol. 2011; 186:1338–1342. [PubMed: 21199897]
25. Mucida D, Husain MM, Muroi S, van Wijk F, Shinnakasu R, Naoe Y, Reis BS, Huang Y, Lambolez F, Docherty M, Attinger A, Shui JW, Kim G, Lena CJ, Sakaguchi S, Miyamoto C, Wang P, Atarashi K, Park Y, Nakayama T, Honda K, Ellmeier W, Kronenberg M, Taniuchi I, Cheroutre H. Transcriptional reprogramming of mature CD4(+) helper T cells generates distinct MHC class II-restricted cytotoxic T lymphocytes. Nat Immunol. 2013; 14:281–289. [PubMed: 23334788]
26. Kim Y, Ponomarenko J, Zhu Z, Tamang D, Wang P, Greenbaum J, Lundegaard C, Sette A, Lund O, Bourne PE, Nielsen M, Peters B. Immune epitope database analysis resource. Nucleic Acids Res. 2012; 40:W525–530. [PubMed: 22610854]
27. Hamilton JA. Colony-stimulating factors in inflammation and autoimmunity. Nat Rev Immunol. 2008; 8:533–544. [PubMed: 18551128]
28. Nemunaitis J. Macrophage function activating cytokines: potential clinical application. Critical reviews in oncology/hematology. 1993; 14:153–171. [PubMed: 8357512]
29. Higgins DM, Sanchez-Campillo J, Rosas-Taraco AG, Higgins JR, Lee EJ, Orme IM, Gonzalez-Juarrero M. Relative levels of M-CSF and GM-CSF influence the specific generation of macrophage populations during infection with Mycobacterium tuberculosis. J Immunol. 2008; 180:4892–4900. [PubMed: 18354213]
30. Jamieson SE, Miller EN, Black GF, Peacock CS, Cordell HJ, Howson JM, Shaw MA, Burgner D, Xu W, Lins-Lainson Z, Shaw JJ, Ramos F, Silveira F, Blackwell JM. Evidence for a cluster of genes on chromosome 17q11-q21 controlling susceptibility to tuberculosis and leprosy in Brazilians. Genes and immunity. 2004; 5:46–57. [PubMed: 14735149]
31. Zhang G, Chen X, Chan L, Zhang M, Zhu B, Wang L, Zhu X, Zhang J, Zhou B, Wang J. An SNP selection strategy identified IL-22 associating with susceptibility to tuberculosis in Chinese. Scientific reports. 2011; 1:20. [PubMed: 22355539]
32. Berry MPR, Graham CM, McNab FW, Xu Z, Bloch SAA, Oni T, Wilkinson KA, Banchereau R, Skinner J, Wilkinson RJ, Quinn C, Blankenship D, Dhawan R, Cush JJ, Mejias A, Ramilo O, Kon OM, Pascual V, Banchereau J, Chaussabel D, O/'Garra A. An interferon-inducible neutrophil-driven blood transcriptional signature in human tuberculosis. Nature. 2010; 466:973–977. [PubMed: 20725040]
33. Maertzdorf J, Ota M, Repsilber D, Mollenkopf HJ, Weiner J, Hill PC, Kaufmann SHE. Functional Correlations of Pathogenesis-Driven Gene Expression Signatures in Tuberculosis. PLoS ONE. 2011; 6:e26938. [PubMed: 22046420]
34. Maertzdorf J, Weiner J, Mollenkopf H-J, Network T, Bauer T, Prasse A, Müller-Quernheim J, Kaufmann SHE. Common patterns and disease-related signatures in tuberculosis and sarcoidosis. Proceedings of the National Academy of Sciences. 2012; 109:7853–7858.
35. Bloom CI, Graham CM, Berry MP, Rozakeas F, Redford PS, Wang Y, Xu Z, Wilkinson KA, Wilkinson RJ, Kendrick Y, Devouassoux G, Ferry T, Miyara M, Bouvry D, Valeyre D, Gorochov G, Blankenship D, Saadatian M, Vanhems P, Beynon H, Vancheeswaran R, Wickremasinghe M, Chaussabel D, Banchereau J, Pascual V, Ho LP, Lipman M, O'Garra A. Transcriptional blood signatures distinguish pulmonary tuberculosis, pulmonary sarcoidosis, pneumonias and lung cancers. PLoS One. 2013; 8:e70630. [PubMed: 23940611]
36. Bloom CI, Graham CM, Berry MP, Wilkinson KA, Oni T, Rozakeas F, Xu Z, Rossello-Urgell J, Chaussabel D, Banchereau J, Pascual V, Lipman M, Wilkinson RJ, O'Garra A. Detectable changes in the blood transcriptome are present after two weeks of antituberculosis therapy. PLoS One. 2012; 7:e46191. [PubMed: 23056259]
37. Kaforou M, Wright VJ, Oni T, French N, Anderson ST, Bangani N, Banwell CM, Brent AJ, Crampin AC, Dockrell HM, Eley B, Heyderman RS, Hibberd ML, Kern F, Langford PR, Ling L, Mendelson M, Ottenhoff TH, Zgambo F, Wilkinson RJ, Coin LJ, Levin M. Detection of tuberculosis in HIV-infected and -uninfected African adults using whole blood RNA expression signatures: a case-control study. PLoS Med. 2013; 10:e1001538. [PubMed: 24167453]
38. Sallusto F, Lanzavecchia A. Heterogeneity of CD4+ memory T cells: Functional modules for tailored immunity. Eur J Immunol. 2009; 39:2076–2082. [PubMed: 19672903]

39. Winslow GM, Cooper A, Reiley W, Chatterjee M, Woodland DL. Early T-cell responses in tuberculosis immunity. Immunol Rev. 2008; 225:284–299. [PubMed: 18837789]
40. Pathan AA, Wilkinson KA, Klenerman P, McShane H, Davidson RN, Pasvol G, Hill AVS, Lalvani A. Direct Ex Vivo Analysis of Antigen-Specific IFN-γ-Secreting CD4 T Cells in Mycobacterium tuberculosis-Infected Individuals: Associations with Clinical Disease State and Effect of Treatment. J Immunol. 2001; 167:5217–5225. [PubMed: 11673535]
41. Kaufmann SH. Protection against tuberculosis: cytokines, T cells, and macrophages. Annals of the rheumatic diseases. 2002; 6(Suppl 2):ii54–58. [PubMed: 12379623]
42. Guzzetta G, Kirschner D. The roles of immune memory and aging in protective immunity and endogenous reactivation of tuberculosis. PLoS One. 2013; 8:e60425. [PubMed: 23580062]
43. Zhang HH, Song K, Rabin RL, Hill BJ, Perfetto SP, Roederer M, Douek DC, Siegel RM, Farber JM. CCR2 identifies a stable population of human effector memory CD4+ T cells equipped for rapid recall response. J Immunol. 2010; 185:6646–6663. [PubMed: 20980630]
44. Hirschhorn-Cymerman D, Budhu S, Kitano S, Liu C, Zhao F, Zhong H, Lesokhin AM, Avogadri-Connors F, Yuan J, Li Y, Houghton AN, Merghoub T, Wolchok JD. Induction of tumoricidal function in CD4+ T cells is associated with concomitant memory and terminally differentiated phenotype. J Exp Med. 2012; 209:2113–2126. [PubMed: 23008334]
45. Streeck H, D'Souza MP, Littman DR, Crotty S. Harnessing CD4(+) T cell responses in HIV vaccine development. Nat Med. 2013; 19:143–149. [PubMed: 23389614]
46. Soghoian DZ, Jessen H, Flanders M, Sierra-Davidson K, Cutler S, Pertel T, Ranasinghe S, Lindqvist M, Davis I, Lane K, Rychert J, Rosenberg ES, Piechocka-Trocha A, Brass AL, Brenchley JM, Walker BD, Streeck H. HIV-specific cytolytic CD4 T cell responses during acute HIV infection predict disease outcome. Sci Transl Med. 2012; 4:123ra125.
47. Chaudhary PM, Roninson IB. Expression and activity of P-glycoprotein, a multidrug efflux pump, in human hematopoietic stem cells. Cell. 1991; 66:85–94. [PubMed: 1712673]
48. Sincock PM, Ashman LK. Expression of c-Kit and functional drug efflux are correlated in de novo acute myeloid leukaemia. Leukemia. 1997; 11:1850–1857. [PubMed: 9369417]
49. Mackay F, Schneider P, Rennert P, Browning J. BAFF AND APRIL: a tutorial on B cell survival. Annu Rev Immunol. 2003; 21:231–264. [PubMed: 12427767]
50. Boniface K, Blumenschein WM, Brovont-Porth K, McGeachy MJ, Basham B, Desai B, Pierce R, McClanahan TK, Sadekova S, de Waal Malefyt R. Human Th17 cells comprise heterogeneous subsets including IFN-gamma-producing cells with distinct properties from the Th1 lineage. J Immunol. 2010; 185:679–687. [PubMed: 20511558]

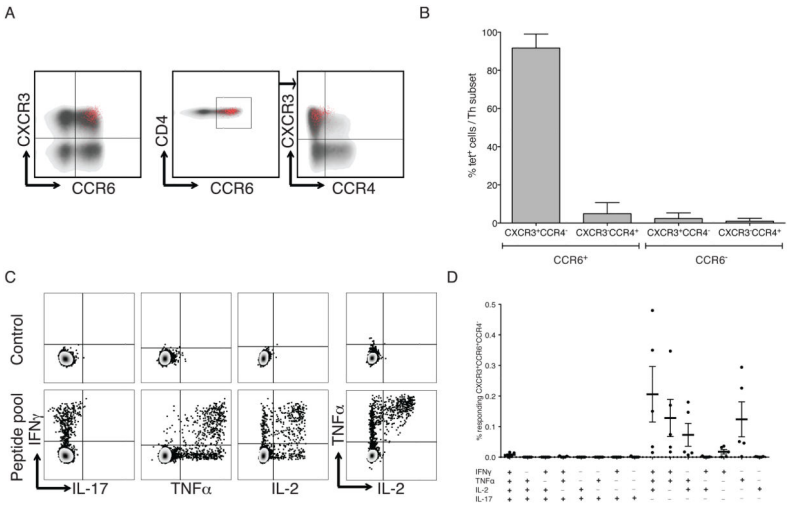

Figure 1. TB-specific memory CD4$^+$ T cells are restricted to the CCR6$^+$CXCR3$^+$CCR4$^-$ subset and produce IFNγ, TNFα and IL-2 but no IL-17

Representative dot plots from one donor. Plots are gated on total CD4$^+$ memory T cells (grey background) or epitope-specific CD4$^+$ memory T cells (red dots) (*A*). Percentage of tetramer$^+$ T cells divided into 4 Th subsets; CCR6$^+$CXCR3$^+$CCR4$^-$, CCR6$^-$CXCR3$^+$CCR4$^-$ (Th1), CCR6$^+$CXCR3$^-$CCR4$^-$ (Th17), and CCR6$^-$CXCR3$^-$CCR4$^+$ (Th2) cells. Data represent median ± interquartile range from 5 donors (*B*). Epitope-specific IFNγ, TNFα, IL-2 and IL-17 production by CCR6$^+$CXCR3$^+$CCR4$^-$ T cells measured after 6 h stimulation. Representative dot plots from one donor. Plots are gated on CCR6$^+$CXCR3$^+$CCR4$^-$ T cells stimulated with media (control, top panel) or peptide pool (bottom panel) (*C*). Percentage of responding CCR6$^+$CXCR3$^+$CCR4$^-$ expressing each of the fifteen possible combinations of IFNγ, TNFα, IL-2 and IL-17. Each dot represents one donor; mean ± SEM is indicated (*D*).

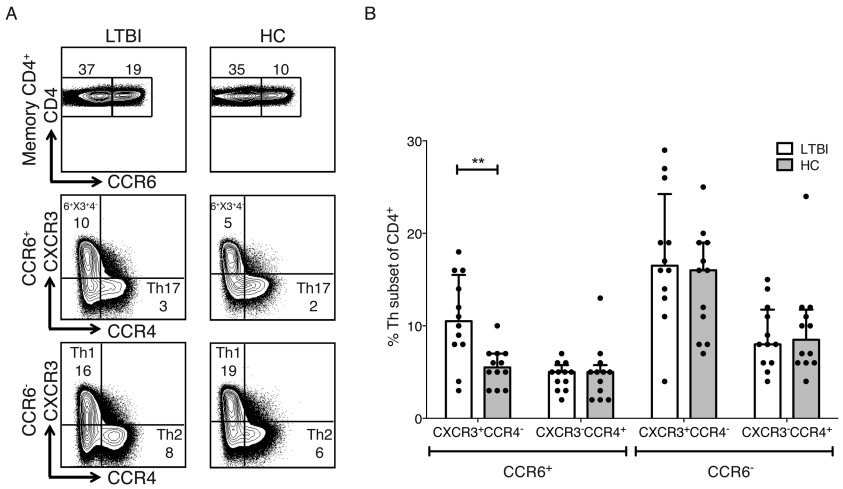

Figure 2. The CCR6^{+}CXCR3^{+}CCR4^{-} subset is increased in subjects with LTBI compared to HC

Contour plots for memory T cells from representative LTBI (left panel) and HC (right panel) gated on CCR6$^{+/-}$ (top panel) and further gated on the 4 Th subsets; CCR6^{+}CXCR3^{+}CCR4^{-} (6^{+}X3^{+}4^{-}), CCR6^{+}CXCR3^{-}CCR4^{-} (Th17) (middle panel), CCR6^{-}CXCR3^{+}CCR4^{-} (Th1), and CCR6^{-}CXCR3^{-}CCR4^{+} (Th2) (bottom panel). Numbers indicate percentage of subset in CD4^{+} T cells (*A*). Percentage of CD4^{+} T cells divided into 4 Th subsets as in (A) comparing LTBI (white bars) and HC (grey bars). Data represent median ± interquartile range from 12 LTBI and 12 HC donors. Mann Whitney test, **, $p<0.01$. Filled circles represent data from individual donors (*B*).

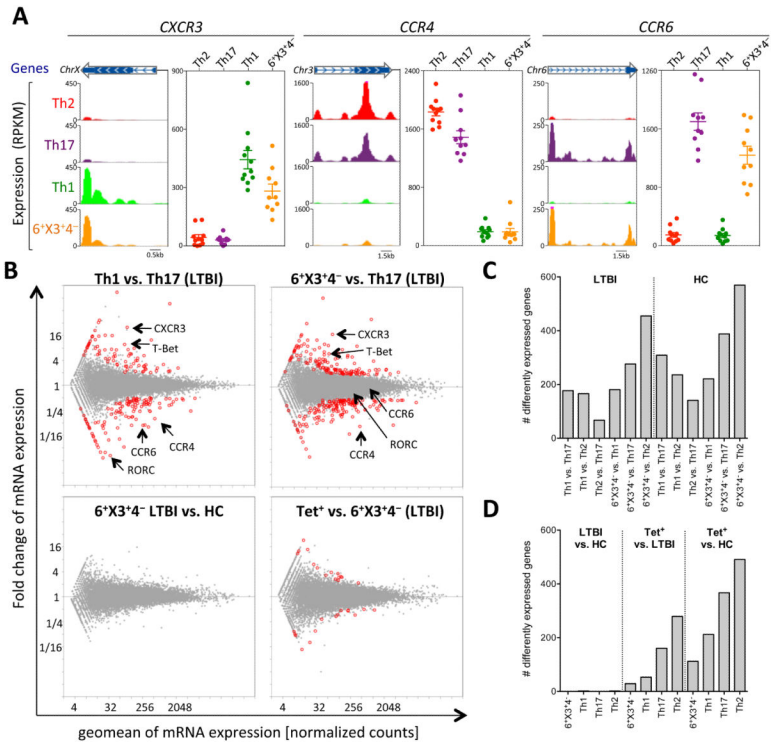

Figure 3. The transcriptional program of TB-specific cells are conserved in the CCR6^{+}CXCR3^{+}CCR4^{-} compartment

Mapping of short mRNA reads to genes encoding CXCR3, CCR4 and CCR6 in Th2 (red), Th1 (green), Th17 (purple) and 6^{+}X3^{+}4^{-} (orange) cells. Dot plots show expression for each individual sample tested. Data represents mean ± SEM (*A*). MA plots comparing gene expression between groups of samples. Geometric mean of expression between the samples (x-axis) is compared to fold change in expression between the samples (y-axis). Differentially expressed genes (red circles) were identified based on having an adjusted p-value < 0.05 according to the DESeq analysis and if they showed an at least 2-fold change in expression. Genes that did not meet these cutoffs were plotted in gray (*B*). Number of differentially expressed genes comparing groups of samples from Th subsets within LTBI and HC donor cohorts (*C*). Number of differentially expressed genes when comparing samples from the same subset between HC vs. LTBI donors and when comparing tetramer positive cells to the different Th subsets (*D*).

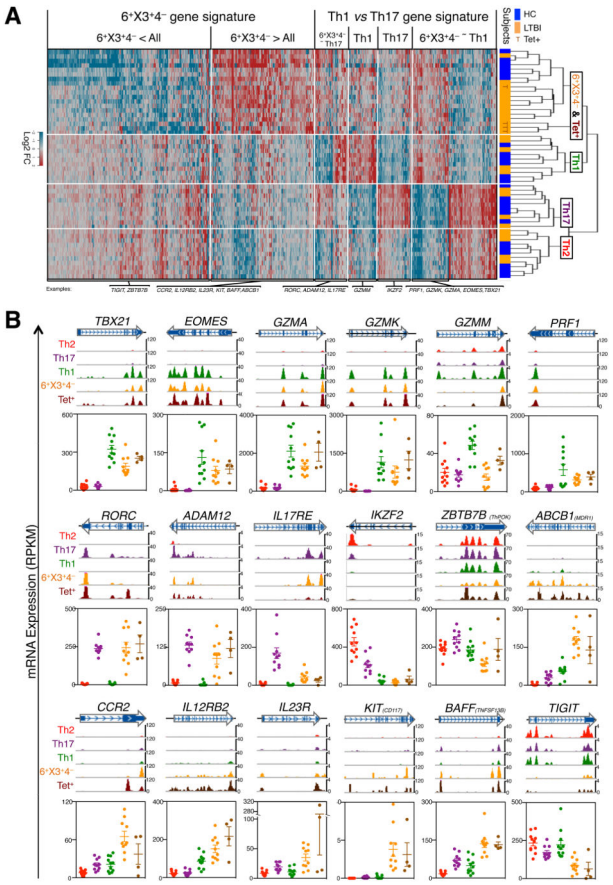

Figure 4. Expression pattern of genes differentially transcribed between sets of samples

Samples from different donors and cell types were clustered based on their similarity in gene expression in the complete set of 1,670 differentially expressed genes. Dendogram showing the sample clustering is shown on the upper right with samples from the same cell type making up the four main clusters. Disease state of the donor of each samples is indicated next to the dendogram (orange = LTBI, blue = HC). The heat map displays expression of each gene (column) as a fold change of the median expression in all samples with blue indicating lower and red indicating higher expression. Selected groups of genes are shown in the heat map: 1) CCR6^{+}CXCR3^{+}CCR4^{-} signature genes (6^{+}X3^{+}4^{-} from LTBI or HC donor being 2-fold higher or 2-fold lower than all other Th subsets from the same donor cohort). 2) Genes that are significantly different in Th1 vs. Th17 samples in either LTBI or HC donors (Th1 vs. Th17 signature), subdivided by into three groups that show either 6^{+}X3^{+}4^{-} expression similar to Th1, 6^{+}X3^{+}4^{-} expression similar to Th17 or 6^{+}X3^{+}4^{-} expression that is intermediate between the two (*A*). Mapping of short mRNA reads to genes differentially expressed in 6^{+}X3^{+}4^{-} (orange), Th1 (green), Th17 (purple), Th2 (red) and Tet^{+} (brown) cells. Dot plots show expression for each individual sample tested. Data represents mean ± SEM (*B*).

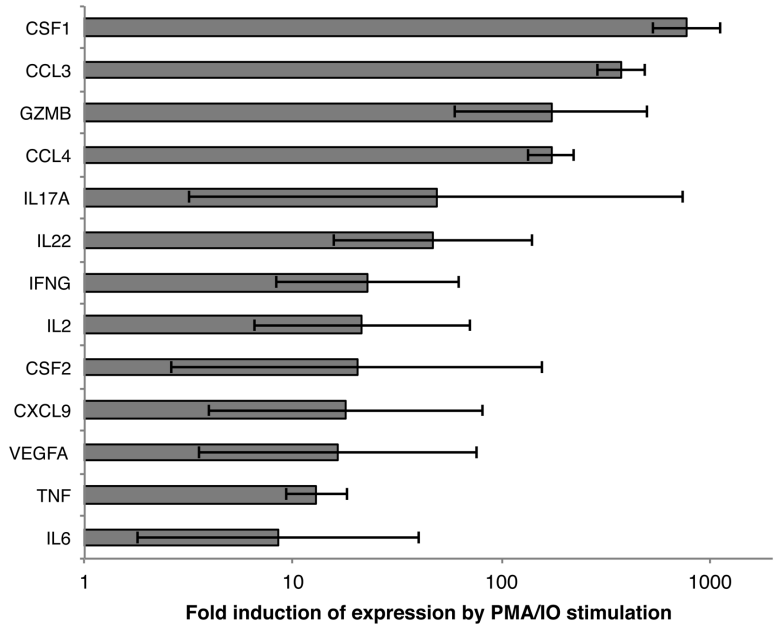

Figure 5. CCR6^{+}CXCR3^{+}CCR4^{-} cells produce a wide range of cytokines after mitogen stimulation

mRNA expression of cytokine genes after stimulation with mitogen compared to the resting state. The cytokines examined were previously described as being produced by human T cells in an epitope-specific manner in PMA/Ionomycin stimulated CCR6^{+}CXCR3^{+}CCR4^{-} cells. Shown are cytokines with at least three-fold induction ranked from highest to lowest. Data represents average ± standard deviation on a log scale for 3 LTBI donors.

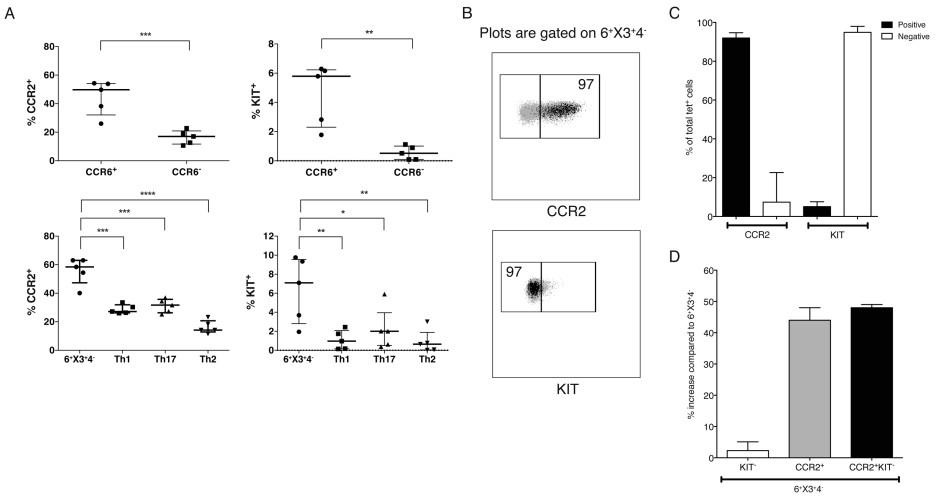

Figure 6. The transcriptional profile of the CCR6$^+$CXCR3$^+$CCR4$^-$ subset is reflected by a similar expression profile of proteins

CD4$^+$ T cells were stained for CCR2 and KIT and expression was compared between different subsets. Top panel; CCR6$^+$ vs. CCR6$^-$, bottom panel; 6$^+$X3$^+$4$^-$, Th1, Th17 and Th2. Each dot represents one donor, median ± interquartile range is indicated. Unpaired one-tailed t test, *, p<0.05, **, p<0.01, ***, p<0.001, ****, p<0.0001 (*A*). CCR2 (top) and KIT (bottom) expression in tet$^+$ CCR6$^+$CXCR3$^+$CCR4$^-$ cells (black dots) compared to CCR6$^+$CXCR3$^+$CCR4$^-$ (grey dots) (*B*). Percentage of tet$^+$ CCR6$^+$CXCR3$^+$CCR4$^-$ cells expressing CCR2 and KIT. Data represent median ± interquartile range from 3 donors (*C*). Percentage increase in tetramer$^+$ cells compared to CCR6$^+$CXCR3$^+$CCR4$^-$ if CCR2$^+$ and/or KIT$^-$ is included in the staining panel. Data represent median ± interquartile range from 3 donors (*D*).